JPPIPA 12(2) (2026)

Jurnal Penelitian Pendidikan IPA

http://jppipa.unram.ac.id/index.php/jppipa/index

# Molecular Mechanisms of *Sechium edule* Based on Network Pharmacology and Molecular Docking on Hypertension

Rahmat Santoso[1], Kintoko[2*], Nining Sugihartini[2]

[1] Fakultas Farmasi, Universitas Bhakti Kencana, Bandung, Indonesia.
[2] Fakultas Farmasi, Ahmad Dahlan University, Yogyakarta, Indonesia.

Received: December 28, 2025
Revised: January 20, 2026
Accepted: March 24, 2026
Published: March 25, 2026

Corresponding Author:
Kintoko
rahmat.santoso@bku.ac.id

DOI: 10.29303/jppipa.v12i2.14114



**Abstract:** Chayote is a fruit that has been used for centuries to treat various diseases, including hypertension. However, how the chemical compounds derived from chayote work in treating hypertension remains unclear. Integrating molecular docking and network pharmacology to elucidate the active constituents and potential mechanisms of chayote in treating hypertension. Initially, 50 active compounds from chayote and 97 key targets related to hypertension were identified through network pharmacology analysis. Then, the results of molecular docking and simulations showed: gibberellin A4; gibberellin A7; gibberellin A29; gibberellin A38; gibberellin A44; stigmasta-3,5-dien-7-one; stigmasterol and routinely overcome hypertension through the regulation of ACE, AKT1, ALB, SRC, and TNF genes. These compounds and genes may be key factors of chayote fruit in treating hypertension. Pathway enrichment analysis showed that the antihypertensive effect of chayote is regulated by the gibberellin A7 and TNF signaling pathways. These pathways are primarily associated with anti-oxidative stress, anti-inflammatory responses, and β-cell protection. This study identified the active constituents and potential signaling pathways involved in the antihypertensive effect of chayote. Result: These findings provide a theoretical basis for understanding the mechanism of the antihypertensive effect of chayote. Furthermore, this study may help develop health supplements or natural antihypertensive drugs based on chayote.

**Keywords:** Hypertension; Mechanism angiotensin-converting enzyme; Molecular docking; Network pharmacology; *Sechium edule*

## Introduction

Hypertension is considered a major cause of global morbidity and mortality and is often associated with metabolic syndrome, vascular dysfunction, and chronic cardiovascular disease (Masenga & Kirabo, 2023; Islam et al., 2024). A network pharmacology approach has been used to construct multi-target interaction networks between bioactive compounds and gene targets in medicinal plant research, allowing for systematic study of molecular mechanisms (Mondal et al., 2025; Tabassum et al., 2022). This disruption, combined with a rise in reactive oxygen species and a decrease in the body's ability to combat them, is known as oxidative stress (Que et al., 2021; Bala et al., 2025). A decline in blood vessel relaxation caused by the endothelium and an increase in vasoconstriction triggered by certain stimuli have been linked to hypertension resulting from oxidative stress (Arista-Ugalde et al., 2022; Zahi et al., 2025). *Sechium edule* (chayote) has been used traditionally as a diuretic and antihypertensive agent, with the fruit, roots, leaves and seeds known to have vascular relaxation and blood pressure lowering effects (Fauziah et al., 2019; Chowdhury et al., 2025).

The antihypertensive effect of root extracts containing cinnamic derivatives such as cinnamic acid methyl ester has been demonstrated through a vasorelaxation effect on an angiotensin II-stimulated rat aorta model, which causes a decrease in blood pressure of up to ± 30mmHg (Lombardo-Earl et al., 2014; Das et al., 2022). Consumption of *Sechium edule* powder in elderly people with metabolic syndrome showed

**How to Cite:**
Santoso, R., Kintoko, & Sugihartini, N. (2026). Molecular Mechanisms of Sechium edule Based on Network Pharmacology and Molecular Docking on Hypertension. *Jurnal Penelitian Pendidikan IPA*, *12*(2), 820-830. https://doi.org/10.29303/jppipa.v12i2.14114

significant reductions in blood pressure, oxidative stress, and inflammation (Tian et al., 2025; Shang et al., 2021), accompanied by improvements in antioxidant status such as SOD and IL-10, and increased HDL-cholesterol after a 6-month treatment period. These effects are attributed to the flavonoid, polyphenol, and cucurbitacin compounds known to have antioxidant, anti-inflammatory, and vasodilatory activities (Al-Khayri et al., 2022).

In further research, a combination of network pharmacology and molecular docking approaches is expected to be used to identify active compounds from *Sechium edule* that modulate hypertension target genes such as ACE, AKT1, eNOS, TNF, and others, as well as to map the biological pathways involved (e.g., antioxidant, anti-inflammatory, and metabolic regulation pathways) (Wu et al., 2014). With this approach, it is hoped that the molecular mechanisms of the interaction of chayote compounds with important signaling pathways can be elucidated more comprehensively, thus supporting the development of health supplements or natural antihypertensive therapies based on this plant.

## Method

*Materials*

*Network Pharmacology*

*Screening of Active Compounds and Targets*

A list of compounds in *Sechium edule* (Chayote) (Jain et al., 2021), plants were compiled based on the analysis of active compounds from previous studies. To generate more comprehensive data, simplified molecular compound structures (SMILES) for each acstive constituent were retrieved from the PubChem database (https://pubchem.ncbi.nlm.nih.gov/). Next, the drug-like properties of each compound were assessed using the Scfbio web server (https://scfbio-iitd.res.in/software/drugdesign/lipinski.jsp) and SwissTargetPrediction (http://www.swisstargetprediction.ch/) to search for related active compound targets based on the SMILES formula (Luo et al., 2023).

*Predicting Hypertension Targets*

A search was conducted on GeneCards (https://www.genecards.org/), each using the keyword "Hypertension," with the aim of identifying targets related to Homo sapiens diseases. From the targets obtained from GeneCards, targets with a relevance score > 1 were selected as potential targets. Next, a Venny 2.1 diagram (https://bioinfogp.cnb.csic.es/tools/venny/) was used to visualize overlapping targets between the selected compounds and hypertension target genes (Luo et al., 2023).

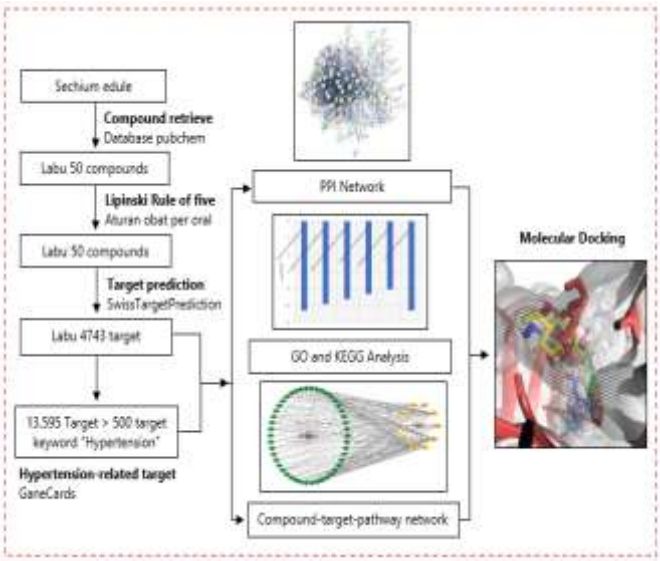


**Figure 1.** The study workflow, consisting of a network pharmacology stage and a validation and prediction stage, aims to elucidate the underlying mechanisms of the antihypertensive effects of chayote

*Protein-Protein Interaction (PPI) Network*

Protein-protein interactions were analyzed using String version 11.0 (https://string-db.org/). To further investigate the mechanism of action of compounds in each plant in the treatment of hypertension, targets were imported into String. The minimum combined score was set to 0.400, and the protein interaction relationships for Homo sapiens were obtained. Targets without interactions were removed, and the data were saved as SIF files. Next, the PPI network was constructed by importing node1, node2, and the combined scores into Cytoscape. Finally, core targets were filtered through cluster analysis using the Cytohubba plug-in in Cytoscape.

*GO and KEGG Pathway Enrichment Analysis*

GO (Gene Ontology) and KEGG pathway analysis were performed using the Metascape website (https://metascape.org/gp/index.html#/main/step1), which is used for the analysis and interpretation of functional genetic or proteomic data, particularly in the context of systems biology and network pharmacology. Biological Process (BP), Cellular Component (CC), and Molecular Function (MF) were selected based on significance ($p < 0.05$). KEGG pathway enrichment analysis was performed to investigate key signaling pathways involved in the hypertension effect.

*Pathway-Gene-Component Network*

To clarify the relationship between active compounds, target genes, and pathways, the top 20 important pathways were intersected with the Pathway-Gene-Disease network to construct a Pathway-Gene-Component network. The results were visualized in Cytoscape.

*In-Silico Test*

The in-silico process was carried out using the molecular docking method. The stages include ligand preparation, protein preparation, validation of the molecular docking method, simulation of the molecular docking of the test ligand with the protein, visualization, and interpretation of the results.

*Ligand Preparation*

The test ligands used were primary plant compounds obtained from the PubChem database (nih.gov). The compounds were downloaded in .sdf format. The ligands were analyzed using the Lipinski rule of five. They were then re-prepared using RDkit software, converting the format to.xyz. The ligand geometry was optimized using eXtended Tight-Binding (XTB) software using the GFN-xTB (Generalized Born–Fock Non-Dynamic Tight-Binding) system, which was developed using GFN 1 and heated to 300 °F (Bursch et al., 2019).

*Protein Preparation*

The target protein used was the hypertension target protein from Network Pharmacology. The 3D file was downloaded from the RCSB Protein Data Bank website (PDB: Homepage) in *.pdb file format. Water molecules and other residues were then removed from the initial structure using Discovery Studio, separating the macromolecule and the natural ligand.

*Molecular Docking*

*Molecular Docking Validation*

Molecular docking validation was performed using AutoDock version 4.2.3 (Morris et al., 2008), the natural ligand, separated from the protein using Discovery Studio, was then redocked onto the target protein. The grid center was located nearly at the center of the ligand, which contains all residues in the binding site. Gridbox determination was performed by setting the central region of the natural ligand and calculating docking with a maximum number of GA runs of 100, a medium number of evaluations, and the Lamarckian Genetic Algorithm (LGA) algorithm. Validation was considered valid if the Root Mean Square Deviation (RMSD) value was ≤ 2Å (Camacho et al., 2016).

*Molecular Docking Simulation*

Molecular docking simulations of the test ligand against the target protein were performed using the Pyrx 0.9.2 application with the Autodock4 algorithm. Gridbox settings were adjusted according to the size and area obtained from the validation results. The next step was to interpret the molecular docking results by examining the ΔG (free energy of binding) values and intermolecular interactions (Akash et al., 2023).

*Molecular Docking Visualization*

To visualize the binding interactions formed between the test ligand and the target protein, we used the applications PLIP (Protein-Ligand Interaction Profiler) Version 2.3.1, DSV (Discovery Studio Visualizer) 2025, and VMD (Visual Molecular Dynamics). Docking visualization depicts the ligand-protein interactions that form intermolecular bonds with amino acid residues (Kolybalov et al., 2024).

## Result and Discussion

Protein target prediction of active compounds in Chayote plants was performed using SwissTargetPrediction, where 50 compounds were analyzed to estimate potential interactions with target proteins. From the initial prediction results, a total of 4743 interactions between compounds and protein targets were obtained. Furthermore, the initial prediction results were sorted based on similarity values, resulting in 801 unique targets retained for further analysis. This filtering process was carried out to eliminate duplications and select targets with a high probability of interaction, so that these targets are expected to have significant potential in pharmacological interactions of active Chayote compounds. Thus, these 801 sorted targets serve as the basis for further studies on the mechanism of action and therapeutic potential of Chayote plants.

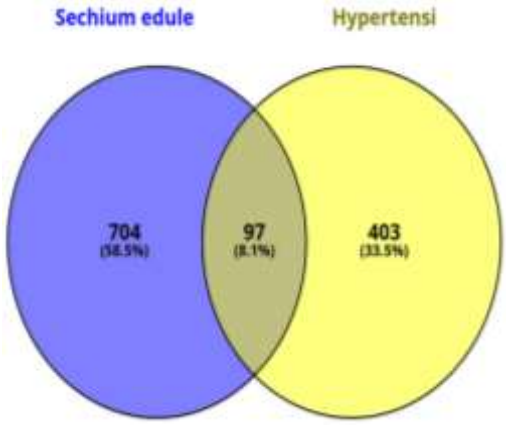


**Figure 2.** Hypertension target overlay results showed that 97 gene targets shared similarities between hypertension targets and those of chayote plants

Prediction of targets involved in hypertension was performed using the GeneCards database. Of the 13,595 gene targets available in the database, the top 500 were selected based on their highest relevance scores to hypertension. This selection was carried out to filter targets most closely related to the molecular mechanisms of the disease, allowing the analysis process to focus on targets considered to have the greatest potential. The relevance score in GeneCards reflects the level of association between a particular gene and the disease based on available scientific evidence (Stelzer et al., 2016). After potential hypertension targets were obtained, an overlay process using Venny was performed to compare these targets with molecular targets obtained from three types of herbal plants, namely Chayote (801 targets). Target data from each plant was obtained from predictions of interactions between active compounds and target proteins, which were previously performed using a network pharmacology approach. Through this process, it was possible to identify which targets are shared by these plants and which are also associated with hypertension.

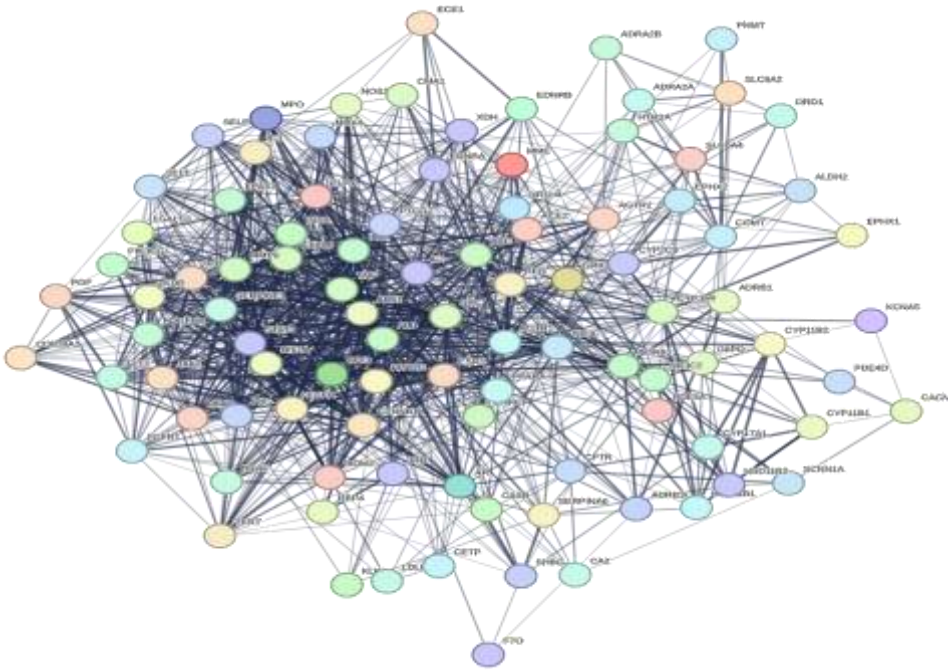

**Figure 3.** Protein-protein interaction-target hypertension. 97 targets were found, and these two plants also form a complex protein interaction network, where several proteins act as key links in the network

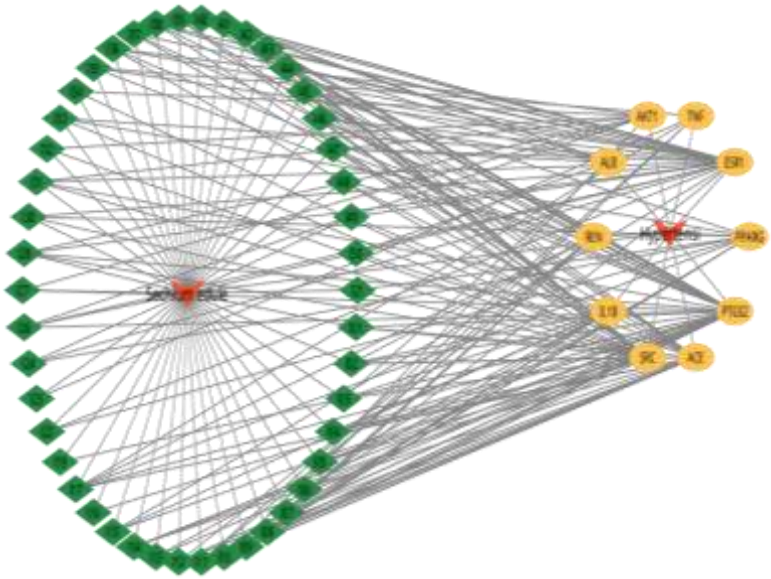

**Figure 4.** Chayote gene-component network—10 key genes occupy central positions in the network. ESR1, SRC, and ACE are of particular interest due to their involvement in hormonal regulation and the renin–angiotensin system, which is closely linked to blood pressure

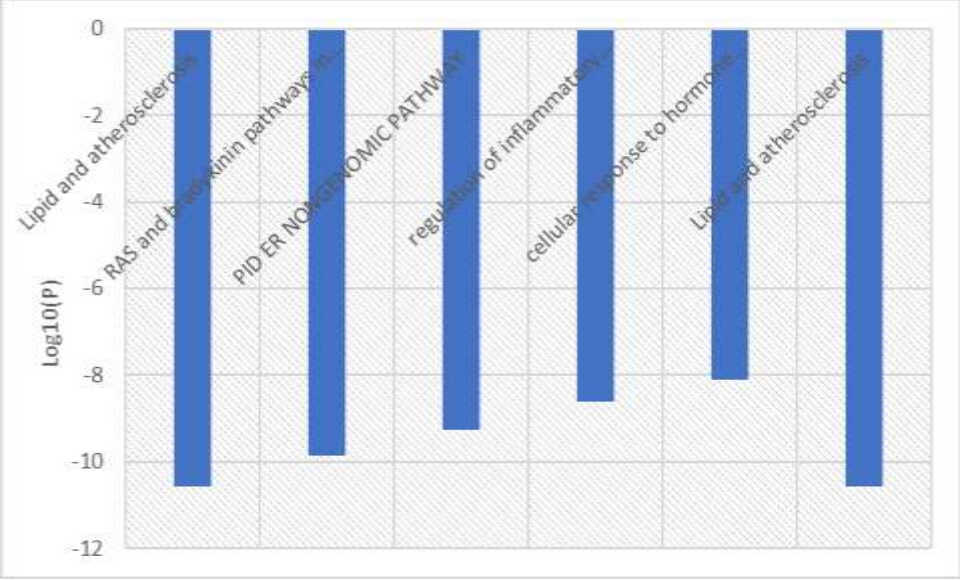


**Figure 5.** GO and KEGG pathway enrichment analysis-chayote pathway "lipid and atherosclerosis" with a total of 6 genes (60%) involved, has a Log10(P) value of -10.59 and a Log10(q) of -6.25

The selection of important targets from the network analysis results was carried out by considering two main parameters, namely Degree and Betweenness Centrality. Targets can be selected as important candidates if they meet the requirements of having a high degree value (in the top 5). Based on previous studies, we set the filtering conditions of Degree > 40 and Betweenness Centrality > 0.024. This indicates that the gene is not only highly connected but also acts as a controlling node or main link. With this approach, the selected targets are considered to have a significant contribution to the stability and biological function of the system.

**Table 1.** Top five chayotes (target *Sechium edule*) based on network analysis using two main parameters, namely degree and betweenness centrality

| Target | PDB code | Gene Symbol | Degree | Betweenness |
|---|---|---|---|---|
| ALB | 2BXD | Serum Albumin | 66 | 537.53 |
| TNF | 7JRA | Tumor Necrosis Factor-α | 62 | 343.70 |
| AKT1 | 3O96 | Protein kinase B | 61 | 381.92 |
| ACE | 1UZF | Angiotensin-Converting Enzyme | 56 | 600.25 |
| SRC | 4MXO | c-Src Tyrosine Kinase | 55 | 729.59 |

The selection of important targets from Chayote (*Sechium edule*) plants has been carried out based on network analysis using two main parameters, namely Degree and Betweenness Centrality, with the condition that the degree value must be more than 40. Degree describes the number of direct connections of a gene in the network, while betweenness centrality shows how often the gene is a link in the information path between other nodes in the biological network. Genes with high values in both parameters are considered as key nodes (hub genes) that play an important role in regulating biological processes and disease pathways such as hypertension. With these findings, the five targets are considered to have a central role in the mechanism of action of the active compounds from the Chayote plant and have great potential for further exploration in the development of natural ingredient-based antihypertensive therapy.

*In-Silico Test*

In the test ligand preparation process, the ligand used was an active compound from the *Sechium edule* (Chayote) plant. The compound was retrieved from the PubChem database and then modeled in 2D and 3D using RdKit software to prepare for Lipinski's rule of five analysis and geometry optimization. Geometry optimization using XTB software using the GFN-xTB (Generalized Born–Fock Non-Dynamic Tight-Binding) method. Geometry optimization using XTB (eXtended Tight-Binding) is based on a semi-empirical approach that combines a tight-binding Hamiltonian with parameterizations for various types of molecules. This method uses the GFN-xTB (Generalized Born–Fock Non-Dynamic Tight-Binding) model that includes dispersion corrections (Grimme's D3/D4) and the option to consider solvent effects through implicit models such as GBSA (Bursch et al., 2022). Optimization is performed by minimizing the total energy of the molecule using an energy gradient, where the energy is calculated from the interactions of electrons and atomic

nuclei in the system. This approach is designed for high efficiency, enabling the analysis of large system geometries with accurate results and much faster computation times than ab initio methods (Lamiable et al., 2016; Romero-Muñiz et al., 2018; Li et al., 2025).

**Table 2.** Active compounds of *Sechium edule* (chayote)

| Code | *Sechium edule* (chayote) | Formula | CID |
|---|---|---|---|
| l01 | Gibberellin A1 | C19H24O6 | 5280379 |
| l02 | Gibberellin A3 | C19H22O6 | 6466 |
| l03 | Gibberellin A4 | C19H24O5 | 92109 |
| l04 | Gibberellin A7 | C19H22O5 | 92782 |
| l05 | Gibberellin A8 | C19H24O7 | 5280607 |
| l06 | Gibberellin A9 | C19H24O4 | 5281984 |
| l07 | Gibberellin A12 | C20H28O4 | 443450 |
| l08 | Gibberellin A13 | C20H26O7 | 10883375 |
| l09 | Gibberellin A15 | C20H26O5 | 25245948 |
| l10 | Gibberellin A17 | C20H26O7 | 5460657 |
| l11 | Gibberellin A19 | C20H26O6 | 5460209 |
| l12 | Gibberellin A25 | C20H26O6 | 14464358 |
| l13 | Gibberellin A27 | C20H26O6 | There isn't any |
| l14 | Gibberellin A29 | C19H24O6 | 14605548 |
| l15 | Gibberellin A38 | C20H25O6 | 25203635 |
| l16 | Gibberellin A44 | C20H26O5 | 5460372 |
| l17 | Gibberellin A53 | C20H28O5 | 440914 |
| l18 | trans-Zeatin | C10H13N5O | 449093 |
| l19 | 9-Ribosyl-trans-zeatin | C15H21N5O5 | 6440982 |
| l20 | Methyl palmitate | C17H34O2 | 8181 |
| l21 | Palmitic acid | C16H32O2 | 985 |
| l22 | Squalene | C30H50 | 638072 |
| l23 | Stigmasta-3,5-dien-7-one | C29H46O | 12444466 |
| l24 | Stigmasterol | C29H48O | 5280794 |
| l25 | Gamma-nonalactone | C9H16O2 | 7710 |
| l26 | Stigmastadiene | C29H48 | 129646093 |
| l27 | Monopalmitin | C19H38O4 | 14900 |
| l28 | Apigenin | C15H10O5 | 5280443 |
| l29 | Catechin | C15H14O6 | 9064 |
| l30 | Hesperetin | C16H14O6 | 72281 |
| l31 | Luteolin | C15H10O6 | 5280445 |
| l32 | Myricetin | C15H10O8 | 5281672 |
| l33 | Naringenin | C15H12O5 | 439246 |
| l34 | Quercetin | C15H10O7 | 5280343 |
| l35 | Rutin | C27H30O16 | 5280805 |
| l36 | Umbelliferone | C9H6O3 | 5281426 |
| l37 | Caffeic acid | C9H8O4 | 689043 |
| l38 | 2,4-dihydroxybenzoic acid | C7H6O4 | 1491 |
| l39 | Chlorogenic acid | C16H18O9 | 1794427 |
| l40 | Ferulic acid | C10H10O4 | 445858 |
| l41 | Gallic acid | C7H6O5 | 370 |
| l42 | Gentisic acid | C7H6O4 | 3469 |
| l43 | o-Coumaric acid | C9H8O3 | 637540 |
| l44 | p-coumaric acid | C9H8O3 | 637542 |
| l45 | p-hydroxybenzoic acid | C7H6O3 | 135 |
| l46 | Protocatechuic acid | C7H6O4 | 72 |
| l47 | Salicylic acid | C7H6O3 | 338 |
| l48 | Syringic acid | C9H10O5 | 10742 |
| l49 | t-cinnamic acid | C9H8O2 | 444539 |
| l50 | Vanillic acid | C8H8O4 | 8468 |

*Molecular Docking*

Molecular docking validation is carried out by molecular docking or known as redocking which is expressed in the form of RMSD (Root Mean Square Deviation) on. The purpose of redocking is to place the original ligand location at the initial location that is validated in the form of the size and position of the gridbox. Molecular docking validation is declared valid if the RMSD value is ≤ 2 Å, meaning that the molecular docking method provides a deviation that is not large and can be used further for simulation of docking of test ligand molecules. This procedure has been widely used as a standard approach in molecular docking studies (Meng et al., 2012).

**Table 3.** Coordinates of the grid box of the target protein chayote

| PDB code | Coordinate | | | Grid box | | | RMSD (Å) |
|---|---|---|---|---|---|---|---|
| | X | Y | Z | X | Y | Z | |
| 2BXD | 38.88 | 38.68 | 51.53 | 54 | 56 | 52 | 1.61 |
| 7JRA | -15.16 | -2.29 | -26.22 | 54 | 56 | 52 | 1.25 |
| 3O96 | 4.90 | -7.09 | 10.86 | 52 | 54 | 52 | 1.15 |
| 1UZF | 40.83 | 34.38 | 44.60 | 54 | 56 | 52 | 0.83 |
| 4MXO | 12.84 | -36.99 | -6.65 | 56 | 56 | 52 | 1.02 |

Molecular docking simulations can analyze the position of a ligand relative to the target and the chemical bonds that occur so that the affinity of a compound for a target can be predicted. Molecular docking simulations for test ligands are carried out to obtain the interaction and affinity of the test ligand to the active site of the target protein. The free binding energy is a measure of the ligand's ability to bind to the target (Holderbach et al., 2020; Hassan et al., 2024). The smaller the free binding energy value, the higher the affinity between the target and the ligand, and vice versa, the larger the free binding energy value, the lower the affinity between the target and the ligand (Yasuda et al., 2022). The free binding energy (ΔG) value indicates the stability of the ligand to bind to the receptor. The more negative the Gbind value, the better the stability level, so that the bond between the ligand and the receptor is stronger. The Ki value indicates the concentration of inhibitor required to inhibit target performance (Syarafina et al., 2022; Sultana & Woo, 2025). Test ligands with inhibition constant values less than 100 μM are considered potent inhibitors, while those with inhibition constant values greater than 100 μM are considered weak inhibitors (Zheng & Polli, 2010; Du et al., 2016). A low binding free energy value indicates a stable ligand-

target complex (Pandey & Adhikari, 2024; Peng et al., 2019).

**Table 4.** Chayote-target molecular docking

| Code | Binding Affinity | | | | |
|---|---|---|---|---|---|
| | ACE (1UZF) | AKT1 (3O96) | ALB(2BXD) | SRC(4MXO) | TNF(7JRA) |
| LIG | -6.42 | -12.02 | -7.48 | -7.47 | -10.84 |
| ctrl | -6.91 | -7.88 | -7.31 | -7.8 | -7.81 |
| l01 | -7.45 | -8.94 | -7.7 | -6.85 | -10.06 |
| l02 | -7.64 | -9.08 | -7.84 | -7.25 | -9.51 |
| l03 | -7.75 | -8.28 | -7.9 | -7.03 | -10.08 |
| l04 | -7.72 | -7.99 | -8.16 | -7.45 | -10.09 |
| l05 | -7.09 | -8.15 | -7.66 | -6.59 | -8.35 |
| l06 | -7.78 | -8.77 | -8.19 | -7.56 | -10.32 |
| l07 | -6.82 | -7.03 | -8.75 | -5.41 | -9.47 |
| l08 | -3.92 | -6.69 | -5.19 | -3.14 | -8.68 |
| l09 | -6.99 | -8.18 | -7.54 | -5.95 | -9.5 |
| l10 | -4.8 | -6.58 | -7.21 | -3.75 | -7.05 |
| l11 | -6.3 | -7.48 | -7.71 | -3.98 | -9.14 |
| l12 | -3.94 | -7.45 | -8.91 | -3.26 | -8.07 |
| l13 | -7.64 | -7.44 | -7 | -6.18 | -8.47 |
| l14 | -7.47 | -8.41 | -8.03 | -6.46 | -9.8 |
| l15 | -8.39 | -8.97 | -8.78 | -8.01 | -10.05 |
| l16 | -7.82 | -8.82 | -8.41 | -6.33 | -10.7 |
| l17 | -7.75 | -7.41 | -7.92 | -6.09 | -9.51 |
| l18 | -5.2 | -5.46 | -5.81 | -4.13 | -5.62 |
| l19 | -4.54 | -6.74 | -4.21 | -3.26 | -4.95 |
| l20 | -4.68 | -4.6 | -3.87 | -3.41 | -6.68 |
| l21 | -4.49 | -5.19 | -4.93 | -3.68 | -5.55 |
| l22 | -6.65 | -8.21 | -5.22 | -5.33 | -9.16 |
| l23 | -9.4 | -11.24 | -9.69 | -9.69 | -10.78 |
| l24 | -8.22 | -10.65 | -8.67 | -8.94 | -10.33 |
| l25 | -5.18 | -5.22 | -4.92 | -4.6 | -5.3 |
| l26 | -9.92 | -10.93 | -10.03 | -9.85 | -11.34 |
| l27 | -3.09 | -4.56 | -3.95 | -4.24 | -5.83 |
| l28 | -6.58 | -7.32 | -6.64 | -6.93 | -8.03 |
| l29 | -7.48 | -7.03 | -6.22 | -6.14 | -7.81 |
| l30 | -6.47 | -7.34 | -6.68 | -6.9 | -7.56 |
| l31 | -6.78 | -7.42 | -6.23 | -7.01 | -8.34 |
| l32 | -5.8 | -6.86 | -5.46 | -7.22 | -7.64 |
| l33 | -6.52 | -6.91 | -6.93 | -5.6 | -7.43 |
| l34 | -6.23 | -7.48 | -6.12 | -7.11 | -7.29 |
| l35 | -5.6 | -8.8 | 1.15 | -3.71 | -2.03 |
| l36 | -5.83 | -5.79 | -5.19 | -5.24 | -5.77 |
| l37 | -5.06 | -5.96 | -4.91 | -5.16 | -4.42 |
| l38 | -4.12 | -4.9 | -4.98 | -3.4 | -3.79 |
| l39 | -6.32 | -5.99 | -6.99 | -5.83 | -6.01 |
| l40 | -4.82 | -5.52 | -5.01 | -4.83 | -4.98 |
| l41 | -3.97 | -4.4 | -4.25 | -3.72 | -4.43 |
| l42 | -4.5 | -4.43 | -4.95 | -3.38 | -3.74 |
| l43 | -4.92 | -6.39 | -5.47 | -4.11 | -5.21 |
| l44 | -5.18 | -6.27 | -5.18 | -4.57 | -5.26 |
| l45 | -4.48 | -4.79 | -4.77 | -3.9 | -4.04 |
| l46 | -3.98 | -5.07 | -4.27 | -3.52 | -4.12 |
| l47 | -4.83 | -4.89 | -4.55 | -3.61 | -3.91 |
| l48 | -4.36 | -5.02 | -5.13 | -4.3 | -4.46 |
| l49 | -5.07 | -6.01 | -5.46 | -4.46 | -5.06 |
| l50 | -4.38 | -4.77 | -4.92 | -3.96 | -4.18 |

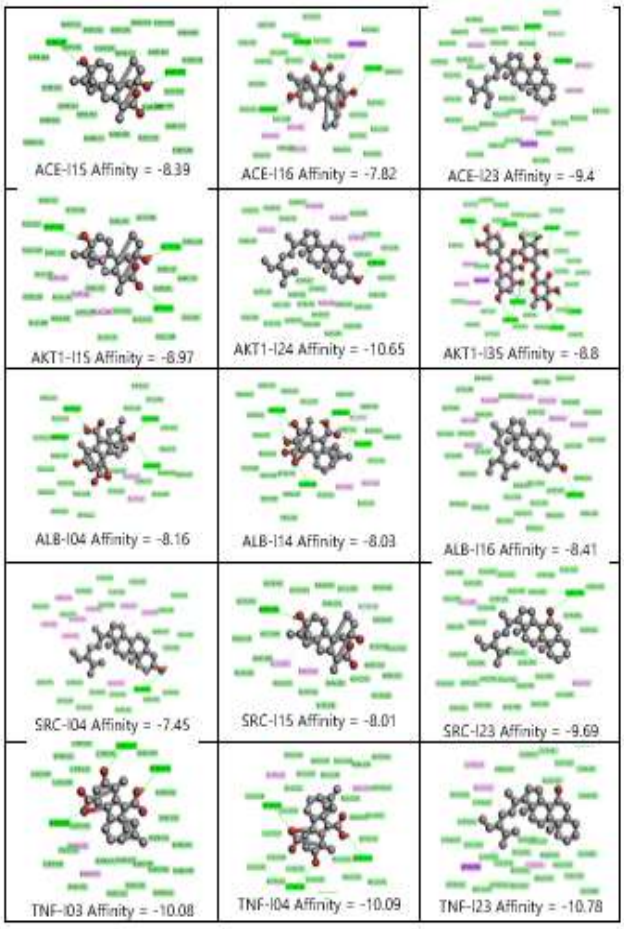


**Figure 6.** Molecular docking visualization between the best compounds chayote-target

The reference compound (LIG) forms six hydrogen bonds and four hydrophobic interactions involving key residues such as Lys511, Tyr520, Gln281, and His513. Hydrophobic interactions involving Ala354, Val380, His353, and His383 also enhance the stability of the formed complex. It can be concluded that this compound has a balanced interaction capability between electrostatic and hydrophobic forces, thus providing good complex stability. Among the tested ligands, compound l15 exhibits strong interactions with six hydrogen bonds and four hydrophobic interactions, involving key residues such as Tyr520. Compound l16 also forms five hydrogen bonds, including Lys511 and Tyr520, but only forms one hydrophobic interaction with Tyr523. Meanwhile, compound l23 forms fewer hydrogen bonds (three) but exhibits a high hydrophobic contribution through five residues, including Tyr523. Based on the involvement of key residues in hydrogen and hydrophobic bonds, compounds l15, l16, and l23 are predicted to have high potential as ACE inhibitor candidates.

The reference ligand (LIG) forms two hydrogen bonds with Glu298 and Ser205, and eight hydrophobic

interactions involving Asp274, Leu264, and Tyr272. The involvement of these key residues suggests that ligand binding can be stabilized through a balanced combination of electrostatic and hydrophobic interactions. The strength and direction of these interactions may optimize the ligand's affinity for AKT1 compared to amlodipine. Among the tested ligands, compound l35 exhibits the most intensive interactions, with nine hydrogen bonds and two hydrophobic interactions involving Ser205, Tyr272, and several additional residues such as Lys268 and Val271. Meanwhile, compound l15 interacts through three hydrogen bonds and five hydrophobic interactions, involving key residues Thr211 and Tyr272. Compound l24 exhibits two hydrogen bonds with Thr211 and Leu213 and five hydrophobic interactions, including Tyr272. Based on the involvement of important residues and the strength of the interactions formed, compound l35 is considered to have the most promising potential as an AKT1 inhibitor, followed by l15 and l24.

The reference ligand (LIG) is known to form three hydrogen bonds with residues Arg257, His242, and Lys199, and eight hydrophobic interactions involving Leu238, Trp214, and Tyr150. Compared to amlodipine, the interactions generated by LIG exhibit a broader residue coverage, including involvement of key residues such as His242, suggesting that the complex can be more effectively stabilized by this ligand. Of the test ligands, compound l16 forms three hydrogen bonds with residues Ala291, Arg222, and Tyr150, and six hydrophobic interactions involving Arg257, Leu238, and Leu260. These interactions involve two of the three key residues, Arg222 and Ala291. Meanwhile, compound l14 forms three hydrogen bonds and four hydrophobic interactions, also involving the key residue Ala291. Compound l04 forms two hydrogen bonds and four hydrophobic interactions with a similar residue involvement pattern. Based on the involvement of important residues and the strength of their interactions, it can be concluded that compound l16 shows the best potential in forming a stable complex with ALB, followed by l14 and l04 (Rahman et al., 2022; Yu et al., 2024).

The reference compound (LIG) formed only one hydrogen bond with residue Met341 and three hydrophobic interactions with Ala293, Leu273, and Leu393. These interactions were more limited compared to the reference drug, although involvement of the crucial residue Met341 was still observed. This suggests that the LIG ligand may form a less stable complex than the other test compounds. Of the test ligand results, compound l04 showed the most comprehensive interactions, with three hydrogen bonds involving Glu339, Met341, and Thr338, and seven hydrophobic interactions, including Ile336 and Val323. Compound l15 formed two hydrogen bonds, one with Met341, and five hydrophobic interactions. Meanwhile, l23 formed one hydrogen bond with Met341 and seven extensive hydrophobic interactions. Based on the involvement of key residues such as Met341, Thr338, and Ile336, it can be concluded that compound l04 has the most potential interaction in forming a stable complex with cSrc Tyrosine Kinase, followed by l23 and l15.

The reference ligand (LIG) forms three hydrogen bonds involving residues Leu233, Tyr195, and Tyr227, and six hydrophobic interactions also involving Ile231 and Tyr135. With the involvement of four key residues (Leu233, Tyr195, and Tyr227), along with the support of other hydrophobic interactions, this ligand exhibits a stronger intermolecular affinity than amlodipine. Of the three test ligands, compounds l03 and l04 exhibit a similar interaction pattern, with one hydrogen bond involving Tyr195 and three hydrophobic interactions with Leu133, Tyr135, and Tyr195. Meanwhile, l23 forms one hydrogen bond with Leu233 and generates six hydrophobic interactions, including indirectly with the key residue Ala232 via Leu233 and Tyr227. Based on the number and position of interactions, it can be concluded that compound l23 has the best interaction affinity with Tumor Necrosis Factor α, followed by the ligand LIG, then l03 and l04.

## Conclusion

The results of molecular docking and simulations showed: gibberellin A4; gibberellin A7; gibberellin A29; gibberellin A38; gibberellin A44; stigmasta-3,5-dien-7-one; stigmasterol and rutin overcome hypertension through the regulation of ACE, AKT1, ALB, SRC, and TNF genes. These compounds and genes may be key factors of chayote fruit in treating hypertension. Pathway enrichment analysis showed that the antihypertensive effect of chayote is regulated by the gibberellin A7 and TNF signaling pathways. These pathways are primarily associated with anti-oxidative stress, anti-inflammatory responses, and β-cell protection. This study identified the active constituents and potential signaling pathways involved in the antihypertensive effect of chayote. Conclusion: These findings provide a theoretical basis for understanding the mechanism of the antihypertensive effect of chayote. Furthermore, this study may help develop health supplements or natural antihypertensive drugs based on chayote.

**Acknowledgments**

Thanks to all parties who have supported the implementation of this research. I hope this research can be useful. The authors sincerely appreciate the institutional support and provision of research facilities from the Faculty of Pharmacy, Bhakti

Kencana University, Bandung, and the Faculty of Pharmacy, Ahmad Dahlan University, Yogyakarta. Special thanks are extended to Kintoko and Nining Sugihartini for the support of this research. We are also grateful to all parties who directly or indirectly contributed to the completion of this manuscript.

**Author Contributions**

Conceptualization, methodology, investigation, resources, data curation, writing—original draft preparation, R.S.; validation, formal analysis, writing—review and editing, visualization, K. and N.S. All authors have read and agreed to the published version of the manuscript.

**Funding**

The research and writing of this article were funded by Direktorat Riset Pengabdian Masyarakat (DRPM) Bhakti Kencana University.

**Conflicts of Interest**

This research has no conflicts of interest.

## References

Akash, S., Bayıl, I., Rahman, M. A., Mukerjee, N., Maitra, S., Islam, M. R., Rajkhowa, S., Ghosh, A., Al-Hussain, S. A., Zaki, M. E. A., Jaiswal, V., Sah, S., Barboza, J. J., & Sah, R. (2023). Target Specific Inhibition of West Nile Virus Envelope Glycoprotein and Methyltransferase Using Phytocompounds: An in Silico Strategy Leveraging Molecular Docking and Dynamics Simulation. *Frontiers in Microbiology*, *14*(June), 1–20. https://doi.org/10.3389/fmicb.2023.1189786

Al-Khayri, J. M., Sahana, G. R., Nagella, P., Joseph, B. V., Alessa, F. M., & Al-Mssallem, M. Q. (2022). Flavonoids as Potential Anti-Inflammatory Molecules: A Review. *Molecules*, *27*(9), 2901. https://doi.org/10.3390/molecules27092901

Arista-Ugalde, T. L., Santiago-Osorio, E., Monroy-García, A., Rosado-Pérez, J., Aguiñiga-Sánchez, I., Cadena-Iñiguez, J., Gavia-García, G., & Mendoza-Núñez, V. M. (2022). Antioxidant and Anti-Inflammatory Effect of the Consumption of Powdered Concentrate of Sechium edule var. Nigrum spinosum in Mexican Older Adults with Metabolic Syndrome. *Antioxidants*, *11*(6), 1–14. https://doi.org/10.3390/antiox11061076

Bala, L., Jeyabalan, S., Veeraraghavan, G., Kaliaperumal, K., Ashok, C., & Pandiyan, D. D. (2025). Exploring Flavonoids as Multi-Target Therapeutic Agents in Alzheimer's Disease: Insights from Network Pharmacology, Molecular Docking, and Dynamics. *Journal of Applied Pharmaceutical Science*, *15*(11). https://doi.org/10.7324/JAPS.2025.v15.i11.12

Bursch, M., Mewes, J., Hansen, A., & Grimme, S. (2022). Best-Practice DFT Protocols for Basic Molecular Computational Chemistry**. *Angewandte Chemie International Edition*, *61*(42), e202205735. https://doi.org/10.1002/anie.202205735

Bursch, M., Neugebauer, H., & Grimme, S. (2019). Structure Optimisation of Large Transition-Metal Complexes with Extended Tight-Binding Methods. *Angewandte Chemie - International Edition*, *58*(32), 11078–11087. https://doi.org/10.1002/anie.201904021

Camacho, L. E., García-Godoy, M. J., García-Nieto, J., Nebro, A. J., & Aldana-Montes, J. F. (2016). A New Multi-Objective Approach for Molecular Docking Based on RMSD and Binding Energy. *Lecture Notes in Computer Science (Including Subseries Lecture Notes in Artificial Intelligence and Lecture Notes in Bioinformatics)*, *9702*, 65–77. https://doi.org/10.1007/978-3-319-38827-4_6

Chowdhury, S., Mitra, P., Chakraborty, P., & Kar, K. (2025). Herbal Antihypertensives: Integrative Perspectives from Traditional Medicine and Clinical Pharmacology Up to 2025. *Clinical Traditional Medicine and Pharmacology*, *6*(4), 200246. https://doi.org/10.1016/j.ctmp.2025.200246

Das, G., Gonçalves, S., Heredia, J. B., Romano, A., Jiménez-Ortega, L. A., Gutiérrez-Grijalva, E. P., Shin, H. S., & Patra, J. K. (2022). Cardiovascular Protective Effect of Cinnamon and Its Major Bioactive Constituents: An Update. *Journal of Functional Foods*, *97*, 105045. https://doi.org/10.1016/j.jff.2022.105045

Du, X., Li, Y., Xia, Y.-L., Ai, S.-M., Liang, J., Sang, P., Ji, X.-L., & Liu, S.-Q. (2016). Insights into Protein–Ligand Interactions: Mechanisms, Models, and Methods. *International Journal of Molecular Sciences*, *17*(2), 144. https://doi.org/10.3390/ijms17020144

Fauziah, N. A., Hidajati, K., & Soejoenoes, A. (2019). The Effect of Chayote Extract (Sechium edule) On Blood Pressure in Pregnant Women with Hypertension. *Indonesian Journal of Medicine*, *4*(3), 266–277. https://doi.org/10.26911/theijmed.v4i3.205

Hassan, A. M., Gattan, H. S., Faizo, A. A., Alruhaili, M. H., Alharbi, A. S., Bajrai, L. H., AL-Zahrani, I. A., Dwivedi, V. D., & Azhar, E. I. (2024). Evaluating the Binding Potential and Stability of Drug-like Compounds with the Monkeypox Virus VP39 Protein Using Molecular Dynamics Simulations and Free Energy Analysis. *Pharmaceuticals*, *17*(12), 1617. https://doi.org/10.3390/ph17121617

Holderbach, S., Adam, L., Jayaram, B., Wade, R. C., & Mukherjee, G. (2020). RASPD+: Fast Protein-Ligand Binding Free Energy Prediction Using Simplified Physicochemical Features. *Frontiers in Molecular Biosciences*, *7*, 601065. https://doi.org/10.3389/fmolb.2020.601065

Islam, Md. S., Wei, P., Suzauddula, M., Nime, I., Feroz, F., Acharjee, M., & Pan, F. (2024). The Interplay of

Factors in Metabolic Syndrome: Understanding Its Roots and Complexity. *Molecular Medicine*, *30*(1), 279. https://doi.org/10.1186/s10020-024-01019-y

Jain, J. R., Manohar, S. H., Roy, T. K., & Satyan, K. B. (2021). Phenolic Acid and Flavonoid Patterns in Twelve Sechium edule Varieties. *Acta Scientific Agriculture*, *5*(4), 34–43. https://doi.org/10.31080/asag.2021.05.0967

Kolybalov, D. S., Kadtsyn, E. D., & Arkhipov, S. G. (2024). Computer Aided Structure-Based Drug Design of Novel SARS-CoV-2 Main Protease Inhibitors: Molecular Docking and Molecular Dynamics Study. *Computation*, *12*(1), 18. https://doi.org/10.3390/computation12010018

Lamiable, A., Thevenet, P., Rey, J., Vavrusa, M., Derreumaux, P., & Tuffery, P. (2016). PEP-FOLD3: Faster Denovo Structure Prediction for Linear Peptides in Solution and in Complex. *Nucleic Acids Research*, *44*(1), W449–W454. https://doi.org/10.1093/nar/gkw329

Li, J., Song, K., & Li, J. (2025). CQPES: A GPU-Aided Software Package for Developing Full-Dimensional Accurate Potential Energy Surfaces by Permutation-Invariant-Polynomial Neural Network. *Chemistry*, *7*(6), 201. https://doi.org/10.3390/chemistry7060201

Lombardo-Earl, G., Roman-Ramos, R., Zamilpa, A., Herrera-Ruiz, M., Rosas-Salgado, G., Tortoriello, J., & Jiménez-Ferrer, E. (2014). Extracts and Fractions from Edible Roots of Sechium edule (Jacq.) Sw. with Antihypertensive Activity. *Evidence-Based Complementary and Alternative Medicine*, *2014*. https://doi.org/10.1155/2014/594326

Luo, W., Deng, J., He, J., Yin, L., You, R., Zhang, L., Shen, J., Han, Z., Xie, F., He, J., & Guan, Y. (2023). Integration of Molecular Docking, Molecular Dynamics and Network Pharmacology to Explore the Multi-Target Pharmacology of Fenugreek Against Diabetes. *Journal of Cellular and Molecular Medicine*, *27*(14), 1959–1974. https://doi.org/10.1111/jcmm.17787

Masenga, S. K., & Kirabo, A. (2023). Hypertensive Heart Disease: Risk Factors, Complications and Mechanisms. *Frontiers in Cardiovascular Medicine*, *10*, 1205475. https://doi.org/10.3389/fcvm.2023.1205475

Meng, X.-Y., Zhang, H.-X., Mezei, M., & Cui, M. (2012). Molecular Docking: A Powerful Approach for Structure-Based Drug Discovery. *Current Computer Aided-Drug Design*, *7*(2), 146–157. https://doi.org/10.2174/157340911795677602

Mondal, S., Ganguly, A., Nandi, A., Das, A., Mondal, S., Mukherjee, S., Pawar, S. D., & Dey, Y. N. (2025). Network Pharmacology and Molecular Docking Reveal Multi-Target Mechanisms of Butea monosperma Stem Bark Extract in Ulcerative Colitis. *Scientific Reports*, *15*(1), 40302. https://doi.org/10.1038/s41598-025-24091-8

Morris, G. M., Huey, R., & Olson, A. J. (2008). UNIT Using AutoDock for Ligand-Receptor Docking. In *Current Protocols in Bioinformatics* (Issue SUPPL. 24). https://doi.org/10.1002/0471250953.bi0814s24

Pandey, A., & Adhikari, A. (2024). Free Energy Calculations Reveal the Interaction and Stability of Ligands in the Vicinity of B-DNA Dodecamer. *Main Group Chemistry*, *23*(1), 89–102. https://doi.org/10.3233/MGC-230031

Peng, C., Wang, J., Yu, Y., Wang, G., Chen, Z., Xu, Z., Cai, T., Shao, Q., Shi, J., & Zhu, W. (2019). Improving the Accuracy of Predicting Protein–Ligand Binding-Free Energy With Semiempirical Quantum Chemistry Charge. *Future Medicinal Chemistry*, *11*(4), 303–321. https://doi.org/10.4155/fmc-2018-0207

Que, W., Chen, M., Yang, L., Zhang, B., Zhao, Z., Liu, M., Cheng, Y., & Qiu, H. (2021). A Network Pharmacology-Based Investigation on the Bioactive Ingredients and Molecular Mechanisms of Gelsemium elegans Benth Against Colorectal Cancer. *BMC Complementary Medicine and Therapies*, *21*(1), 99. https://doi.org/10.1186/s12906-021-03273-7

Rahman, Md. M., Islam, Md. R., Akash, S., Mim, S. A., Rahaman, Md. S., Emran, T. B., Akkol, E. K., Sharma, R., Alhumaydhi, F. A., Sweilam, S. H., Hossain, Md. E., Ray, T. K., Sultana, S., Ahmed, M., Sobarzo-Sánchez, E., & Wilairatana, P. (2022). In Silico Investigation and Potential Therapeutic Approaches of Natural Products for COVID-19: Computer-Aided Drug Design Perspective. *Frontiers in Cellular and Infection Microbiology*, *12*, 929430. https://doi.org/10.3389/fcimb.2022.929430

Romero-Muñiz, C., Nakata, A., Pou, P., Bowler, D. R., Miyazaki, T., & Pérez, R. (2018). High-Accuracy Large-Scale DFT Calculations Using Localized Orbitals in Complex Electronic Systems: The Case of Graphene–Metal Interfaces. *Journal of Physics: Condensed Matter*, *30*(50), 505901. https://doi.org/10.1088/1361-648X/aaec4c

Shang, C., Lin, H., Fang, X., Wang, Y., Jiang, Z., Qu, Y., Xiang, M., Shen, Z., Xin, L., Lu, Y., Gao, J., & Cui, X. (2021). Beneficial Effects of Cinnamon and Its Extracts in the Management of Cardiovascular Diseases and Diabetes. *Food & Function*, *12*(24), 12194–12220. https://doi.org/10.1039/D1FO01935J

Stelzer, G., Rosen, N., Plaschkes, I., Zimmerman, S., Twik, M., Fishilevich, S., Iny Stein, T., Nudel, R., Lieder, I., Mazor, Y., Kaplan, S., Dahary, D.,

Warshawsky, D., Guan-Golan, Y., Kohn, A., Rappaport, N., Safran, M., & Lancet, D. (2016). The GeneCards Suite: From Gene Data Mining to Disease Genome Sequence Analyses. *Current Protocols in Bioinformatics*, *2016*(June), 1.30.1-1.30.33. https://doi.org/10.1002/cpbi.5

Sultana, A., & Woo, J. (2025). Structure-Based Identification of Potent Modulators from Centella asiatica Targeting BACE-1. *Heliyon*, *11*(6), e42652. https://doi.org/10.1016/j.heliyon.2025.e42652

Syarafina, Z. Y. I., Safithri, M., Bintang, M., & Kurniasih, R. (2022). In Silico Screening of Cinnamon (Cinnamomum burmannii) Bioactive Compounds as Acetylcholinesterase Inhibitors. *Jurnal Kimia Sains dan Aplikasi*, *25*(3), 97–107. https://doi.org/10.14710/jksa.25.3.97-107

Tabassum, S., Khalid, H. R., Haq, W. U., Aslam, S., Alshammari, A., Alharbi, M., Rajoka, M. S. R., Khurshid, M., & Ashfaq, U. A. (2022). Implementation of System Pharmacology and Molecular Docking Approaches to Explore Active Compounds and Mechanism of Ocimum Sanctum against Tuberculosis. *Processes*, *10*(2), 298. https://doi.org/10.3390/pr10020298

Tian, Y., Jiang, X., Guo, J., Lu, H., Xie, J., Zhang, F., Yao, C., & Hao, E. (2025). Pharmacological Potential of Cinnamic Acid and Derivatives: A Comprehensive Review. *Pharmaceuticals*, *18*(8), 1141. https://doi.org/10.3390/ph18081141

Wu, C. H., Ou, T. T., Chang, C. H., Chang, X. Z., Yang, M. Y., & Wang, C. J. (2014). The Polyphenol Extract from Sechium edule Shoots Inhibits Lipogenesis and Stimulates Lipolysis Via Activation of AMPK Signals in HepG2 Cells. *Journal of Agricultural and Food Chemistry*, *62*(3), 750–759. https://doi.org/10.1021/jf404611a

Yasuda, I., Endo, K., Yamamoto, E., Hirano, Y., & Yasuoka, K. (2022). Differences in Ligand-Induced Protein Dynamics Extracted from an Unsupervised Deep Learning Approach Correlate with Protein–Ligand Binding Affinities. *Communications Biology*, *5*(1), 481. https://doi.org/10.1038/s42003-022-03416-7

Yu, H., Xue, L., Xue, Y., Lu, H., Liu, Y., Wang, L., Du, C., & Liu, W. (2024). Mapping the Structure and Chemical Composition of MAX Phase Ceramics for Their High-Temperature Tribological Behaviors. *Carbon Energy*, *6*(11), e597. https://doi.org/10.1002/cey2.597

Zahi, A., Rani, A., Aktary, N., Rahman, M., Mekhfi, H., Ziyyat, A., Park, M. N., Legssyer, A., & Kim, B. (2025). Cardiovascular Effects, Phytochemistry, Drug Interactions, and Safety Profile of Foeniculum vulgare Mill. (Fennel): A Comprehensive Review. *Pharmaceuticals*, *18*(11), 1761. https://doi.org/10.3390/ph18111761

Zheng, X., & Polli, J. (2010). Identification of Inhibitor Concentrations to Efficiently Screen and Measure Inhibition Ki Values Against Solute Carrier Transporters. *European Journal of Pharmaceutical Sciences*, *41*(1), 43–52. https://doi.org/10.1016/j.ejps.2010.05.013